Synthesis, Structure, and Reactivity of Low-Spin Cobalt(II) Imido Complexes [(Me$_3$P)$_3$Co(NAr)]

Yang Liu,[ID] Jingzhen Du,[ID] and Liang Deng*[ID]

State Key Laboratory of Organometallic Chemistry, Shanghai Institute of Organic Chemistry, University of Chinese Academy of Sciences, Chinese Academy of Sciences, 345 Lingling Road, Shanghai 200032, P. R. China

S *Supporting Information*

ABSTRACT: The reactions of [Co(PMe$_3$)$_4$] with the bulky organic azides, DippN$_3$ and DmpN$_3$ [Dipp, 2,6-diisopropylphenyl; Dmp, 2,6-di(2′,4′,6′-trimethylphenyl)phenyl], afforded the cobalt(II) terminal imido complexes [(Me$_3$P)$_3$Co(NAr)] (Ar = Dipp, **1**; Dmp, **2**). The cobalt imido complexes in their solid states show trigonal pyramidal coordination geometry and long Co−N(imido) separations (ca. 1.71 Å). Spectroscopic characterization and theoretical studies indicated their low-spin cobalt(II) nature. Reactivity studies on **1** revealed its nitrene-transfer reactions with PMe$_3$ and CO, the imido/oxo and imido/sulfido exchange reactions with PhCHO and CS$_2$, and the single-electron oxidation reaction by ferrocenium cation to form cobalt(III) imide.
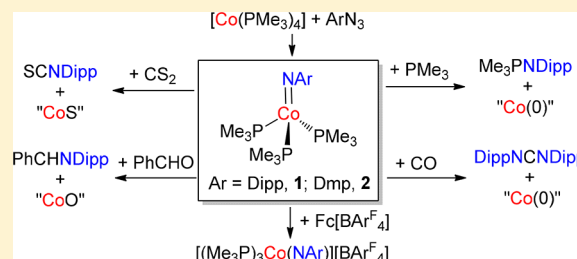
INTRODUCTION

Cobalt imides attract great interest for their role as key intermediates in cobalt-catalyzed nitrene-transfer reactions.[1,2] As is typical of late transition-metal species featuring metal−ligand multiple bonds, the high 3d-electron counting of cobalt could render the occupation of electrons on Co (3d)−N (2p) π* orbitals.[1] Consequently, cobalt imido complexes of the terminal type are reactive, and the reported isolable cobalt imides have to rely on the use of bulky ancillary ligands and bulky substituents on imido to achieve kinetic stabilization. Chart 1 summarizes the reported isolable examples.[3,4] Among them, cobalt(III) imides supported by tripodal and bidentate ligands are dominating (**A**−**H** in Chart 1).[3] These cobalt(III)

Chart 1. Examples of Isolable Cobalt Imido Complexes

imides were synthesized from the reactions of cobalt(I) precursors with organic azides, except **D** that was obtained from hydrogen-atom abstraction of a cobalt(II) amide precursor by phenoxy radical.[3g] It is noteworthy that the reactivity of the cobalt(III) imides remains poorly understood. Nitrene transfer to CO[3a,e] or carbene ligand[3c] to form isocyanates and guanidinate, respectively, was known for **A**, **B**, and **C**. C−H bond activation of ligand was observed on **B** and **H**, in which thermal-induced decomposition of **B** rendered nitrene-insertion into a C−H bond of the Bu^t groups to form cobalt(I) product[3e] and the decomposition of **H** led to benzylic C−H activation of the mesityl group, producing a cobalt(III) cycloindoline.[3i] Both **B** and **H** have thermally accessible open-shell states (S = 1 and 2, respectively). The other cobalt(III) imides are low-spin and diamagnetic.

The syntheses of the first cobalt(II),[4a,b] cobalt(IV),[4c] and cobalt(V)[4c] imido complexes (**I**−**K** in Chart 1) were achieved recently by using monodentate N-heterocyclic carbene (NHC) as ancillary ligand. The cobalt(II) and cobalt(IV) imides were prepared from the reactions of three-coordinate NHC-cobalt(0)-bis(olefin) precursors with 1 and 2 equiv of organic azides, respectively, and the cobalt(V) complex was obtained from one-electron oxidation of cobalt(IV) bis(imide). The formal cobalt(IV) and cobalt(V) complexes have low-spin ground states (S = 1/2 and 0, respectively). Interestingly, the cobalt(IV) imide undergoes intramolecular C−H bond amination at 50 °C, whereas the cobalt(V) species is stable under similar conditions.[4c] The two-coordinate cobalt(II) imido complex has an S = 3/2 ground state and displays slow magnetic relaxation behavior.[4a,b] It shows nitrene-transfer
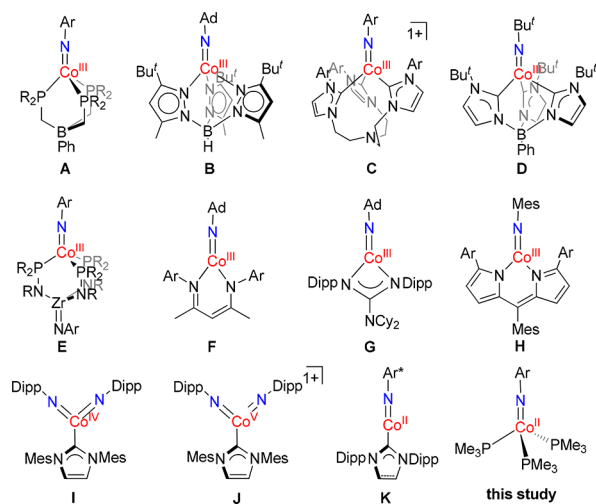
reactivity toward CO and ethylene and can also perform $[2\pi + 2\sigma]$-addition with $C(sp)-H$ and $H-Si$ bonds.[4a] In addition to these studies, we wish to report herein the synthesis, characterization, and reactivity of low-spin cobalt(II) terminal imido complexes in the form of $[(Me_3P)_3Co(NAr)]$. These four-coordinate complexes are the first examples of low-spin cobalt(II) imides. They exhibit nitrene-transfer and imido/oxo(sulfido) exchange reactivity toward CO, PMe_3, CS_2, PhCHO, etc., as shown below.

■ RESULTS AND DISCUSSION

Preparation and Characterization of the Cobalt(II) Imido Complexes. Inspired by the success of using NHC-cobalt(0)-bis(olefin) as cobalt precursors in the synthesis of cobalt imides,[4] we examined the reactions of the cobalt(0) phosphine complex $[(Me_3P)_4Co]$ with organic azides, which also proved to be an effective cobalt(0) precursor to access cobalt imides. The reaction of $[(Me_3P)_4Co]$ with $DippN_3$ (Dipp: 2,6-diisopropylphenyl, 2 equiv) in Et_2O took place at room temperature, leading to the quick formation of dark green solution and effervescence of dinitrogen. Further workup on the reaction mixture upon recrystallization gave the cobalt(II) imido complex $[(Me_3P)_3Co(NDipp)]$ (**1**) in 74% isolated yield as a black crystalline solid and the iminophosphine $Me_3PNDipp$ in 71% yield as a light yellow crystalline solid (Scheme 1). The

Scheme 1. Synthesis of Low-Spin Cobalt(II) Imides
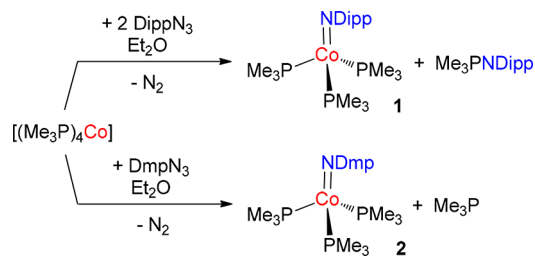
equimolar reaction of $[(Me_3P)_4Co]$ with $DippN_3$ gave a mixture of $[(Me_3P)_4Co]$, **1**, and $Me_3PNDipp$. In contrast, the reaction of $[(Me_3P)_4Co]$ with 1 equiv of $DmpN_3$ [Dmp: 2,6-di(2′,4′,6′-trimethylphenyl)phenyl] could furnish the imido complex $[(Me_3P)_3Co(NDmp)]$ (**2**) in high yield (81%) without noticeable formation of Me_3PNDmp (Scheme 1). As control experiments showed that, while both $DippN_3$ and $DmpN_3$ can react with Me_3P at room temperature to produce the corresponding iminophosphine (Figures S11 and S12),[5] the interaction of **1** with an excess amount of Me_3P gives $Me_3PNDipp$ (*vide infra*), whereas **2** is inert toward Me_3P at ambient conditions. We reason that the iminophosphine $Me_3PNDipp$ formed in the equimolar reaction of $[(Me_3P)_4Co]$ with $DippN_3$ should be formed via the interaction of **1** with PMe_3 with the five-coordinate species $(Me_3P)_4Co(NDipp)$ as a probable intermediate. In the case of the reaction of $[(Me_3P)_3Co(NDmp)]$ with Me_3P, the steric encumbrance of Dmp might make a similar five-coordinate intermediate difficult to form.

Complexes **1** and **2** are air- and moisture-sensitive. In solid states, they are stable at room temperature under a N_2 atmosphere. In C_6D_6, the solution of **1** shows partial decomposition in 1 week to give $Me_3PNDipp$, $[(Me_3P)_4Co]$, and unidentified cobalt species, whereas no decomposition was noticed when the solution of **2** stood at room temperature for

days. Complexes **1** and **2** have been characterized by ^1H NMR, solution magnetic susceptibility measurements, absorption spectroscopy, elemental analyses, X-band EPR spectroscopy, and single-crystal X-ray diffraction studies. The solid-state structures of **1** and **2** (Figure 1 and Figure S1, respectively)
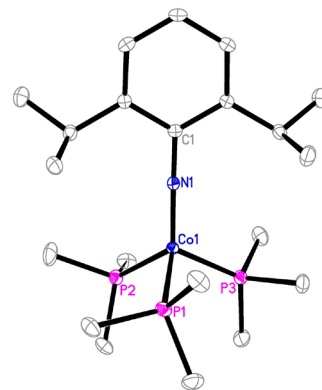
Figure 1. Molecular structure of $[(Me_3P)_3Co(NDipp)]$ (**1**) with 30% probability ellipsoids. Selected distances (Å) and angles (deg): Co1−N1 1.7089(15), Co1−P1 2.2445(6), Co1−P2 2.1814(6), Co1−P3 2.1543(6), N1−C1 1.348(2), Co1−N1−C1 177.85(14), P1−Co1−N1 108.87(6), P2−Co1−N1 124.63(5), P3−Co1−N1 119.16(5), P1−Co1−P2 101.60(2), P1−Co1−P3 101.83(2), P2−Co1−P3 97.38(2).

feature unique distorted trigonal pyramidal CoP_3N cores with the corresponding τ_4 values[6] of 0.82 and 0.80, being close to the τ_4 values of 0.85 for a standard trigonal pyramidal.[6] The displacements of the cobalt centers toward the basal planes (P2−P3−N1) in **1** and **2** are 0.491 and 0.436 Å, respectively. The Co−N−C alignment of the imido moiety in **1** is nearly linear (177.9(1)°), and slightly bent in **2** (161.9(2)°). The Co−N separations (1.709(2) Å and 1.717(2) Å for **1** and **2**, respectively) are longer than those of the cobalt(III) imides **A**−**E** (1.609(3)−1.683(2) Å),[3a−c,e−g,j] consistent with their formal cobalt(II) nature. Despite their distorted trigonal pyramidal geometry in the solid state, the PMe_3 ligands in **1** and **2** only show one ^1H NMR signal, implying the presence of a dynamic process in the solution phase. The X-band EPR spectrum of **1** in toluene glass measured at 1.8 K is characterized by a nearly isotropic g factor (g_{av} = 2.03) with a complex superhyperfine splitting pattern (Figure 2), probably caused by the ^{59}Co (I = 7/2), ^{14}N (I = 1), and ^{31}P (I = 1/2) nuclei. The g value and
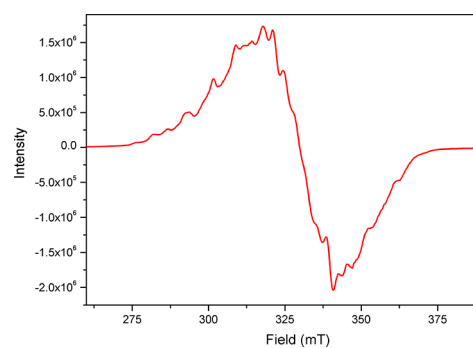
Figure 2. EPR spectrum of $[(Me_3P)_3Co(NDipp)]$ (**1**) recorded in a frozen toluene solution at 1.8 K. Instrumental parameters: ν = 9.387 GHz, modulation frequency = 100 kHz, modulation amplitude = 2 G, microwave power = 0.0502 mW, conversion time = 40.00 ms, time constant = 81.92 ms, sweep time = 240.0 s.

complex superhyperfine pattern are similar to those of Peters' low-spin cobalt(II) complex [PhB(CH$_2$PPh$_2$)$_3$CoI].[7] The measured solution magnetic moments of **1** and **2** (1.9(1) and 2.1(1) μ_B in C$_6$D$_6$ at room temperature)[8] are also indicative of their common S = 1/2 ground state.

In accordance with the low-spin ground state indicated by the experimental data, spin-unrestricted DFT calculations at the B3LYP level using TZVP/SVP basis sets[5] based on the structure of **1** suggested that the single-point energy of **1** at the S = 1/2 state is lower in energy than that of the S = 3/2 state by 16.8 kcal/mol. Analyzing the composition of the frontier molecular orbitals revealed a $(\pi_{xz})^2(\pi_{xy})^2(d_{x^2-y^2})^2(d_{z^2})^2(d_{yz})^2(\pi^*_{xz})^1(\pi^*_{xy})^0$ electronic configuration (Figure 3). The comparable Co 3d and N 2p
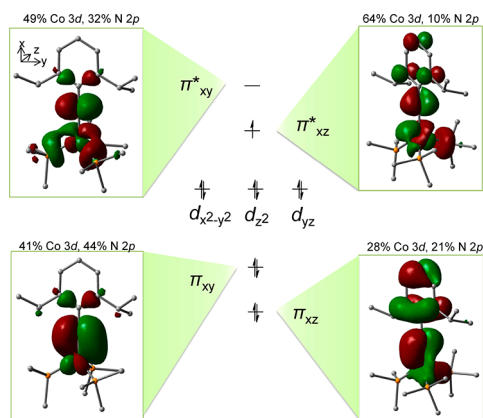

Figure 3. Qualitative frontier molecular orbital diagram of [(Me$_3$P)$_3$-Co(NDipp)] (**1**) at its S = 1/2 state, based on its UHF natural orbitals.

contributions in the in-plane π-interactions (π_{xy} and π^*_{xy}) indicate its high covalency. On the other hand, the relatively high Co 3d orbital and imido orbital content in π^*_{xz} and π_{xz}, respectively, suggests the polarity of the out-of-plane π-bonding. The difference between the two π-interactions should be rooted in the delocalization of the out-of-plane N 2p lone pair to the arene π^*-orbital. In addition, the unique trigonal pyramidal coordination geometry of the cobalt center might also play a role. These Co 3d−N 2p π-interactions render the Co−N multiple bond nature, which has the Mayer bond order of 1.38, much larger than those of the Co−P bonds (0.67−0.80).[5]

Reactivity of the Cobalt(II) Imido Complexes. As mentioned earlier, while plenty of isolable cobalt imido complexes are known, their reactivity has remained poorly understood. With the low-spin cobalt(II) imides in hand, we then explored their reactivity.

The formation of Me$_3$PNDipp in the preparation of **1** implies the nitrene-transfer reactivity of the low-spin cobalt imido complex toward Me$_3$P. Indeed, the reactivity was confirmed by an NMR-scale reaction of **1** with an excess amount of Me$_3$P at room temperature, which gave Me$_3$PNDipp and the cobalt(0) species [Co(PMe$_3$)$_4$] in high yields (Scheme 2). In addition to PMe$_3$, the interaction of the electron-deficient olefin dimethyl fumarate with **1** could also trigger the formation of Me$_3$PNDipp, along with the cobalt(0) complex [(Me$_3$P)$_3$Co-(η^2-(E)-MeO$_2$CCH═CHCO$_2$Me)] (**3**). Figure S10 shows the ^{1}H NMR spectra. The molecular structure of **3** has been established by a single-crystal X-ray diffraction study (Figure

Scheme 2. Reactions of 1 with PMe$_3$, CO, and Olefin
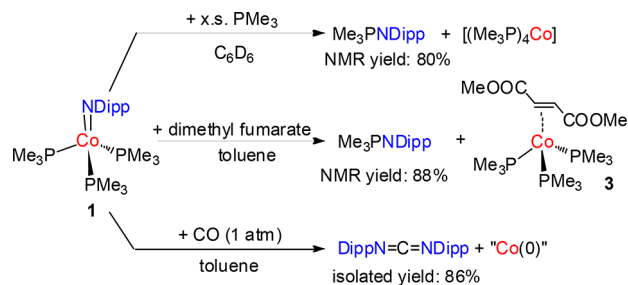
S2), and the structure was refined as a two-component inversion twin giving a Flack parameter of 0.68(3). On the other hand, **1** is inert toward the electron-richer olefins styrene and 1-octene. The conversion of the cobalt(II) imido complex to Me$_3$PNDipp and the cobalt(0) species draws a parallel to ligand-coordination-induced C−C bond-forming reductive elimination reactions of organo-transition-metal compounds.[9] Consequently, we propose that five-coordinate species (Me$_3$P)$_3$(L)Co(NDipp) (L = PMe$_3$, dimethyl fumarate) might be the intermediates en route to the iminophosphine and cobalt(0) species.

Complex **1** can readily undergo nitrene-transfer reaction with CO at room temperature to give the carbodiimide DippNCN-Dipp in high yield (86%, based on **1**) (Scheme 2). This reaction forms a sharp contrast to the slow reaction of Peters' [PhB(CH$_2$PPh$_2$)$_3$Co(N(tolyl))] with CO (70 °C, 14 days) that produced isocyanate, rather than carbodiimide.[3a] The slow rate of the latter reaction might be due to steric effect as the cobalt(III) imido moiety is buried in the pocket of the tripodal ligand. As late transition-metal imido complexes usually react with CO to produce isocyanates,[1,3a,e,4a,10] the formation of the carbodiimide in the current system is unique. The reaction might involve DippNCO, formed from the interaction of **1** with CO (step 1 in Scheme 3), as an intermediate. Once formed, the

**Scheme 3. Possible Routes for the Formation of Carbodiimide from the Reaction of 1 with CO**
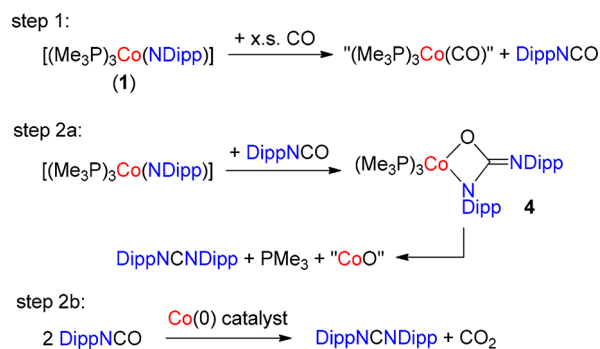
isocyanate might then react with 1 equiv of **1** to form a urinate intermediate (Me$_3$P)$_3$Co(κ^2-N(Dipp)C(NDipp)O) (**4**) that could further convert to DippNCNDipp via retro-[$2\pi + 2\pi$]-addition (step 2a in Scheme 3).[11] As the solution of **4**, which was synthesized from the reaction of **1** with DippNCO (vide infra), does not show decomposition either by itself or under a CO atmosphere, the proposed route (step 2a) seems less likely. Alternatively, noting the capability of certain metal carbonyls in catalyzing the conversion of isocyanates into carbodiimides and CO$_2$,[12] we propose that the carbodiimide might be formed

from low-valent cobalt species-catalyzed disproportionation of the isocyanate (step 2b in Scheme 3).

Examining the reactivity of **1** toward unsaturated polar organic substrates revealed its imido/oxo and imido/sulfido exchange reactions with benzaldehyde and CS_2, respectively (Scheme 4). Both reactions occurred readily at room

Scheme 4. Reactions of 1 with PhCHO, CS$_2$, and DippNCO, and Their Probable Intermediates
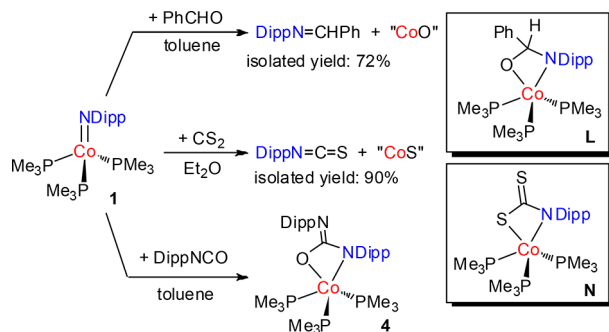
temperature, and gave the imine DippNCHPh and isothiocyanate DippNCS in 72% and 90% yields, respectively. The imine and isothiocyanate might result from retro-cycloaddition reaction of four-membered metallacycles (**L** and **N** in Scheme 4) formed from the $[2\pi + 2\pi]$ cycloaddition of **1** with benzaldehyde and CS_2, along with cobalt(II) oxide and cobalt(II) sulfide as byproducts.[13] While the attempts to isolate the cobalt intermediates were unsuccessful, a five-coordinate cobalt(II) complex bearing an *N,O*-urinate chelate, $[(Me_3P)_3Co(\kappa^2\text{-}N(Dipp)C(NDipp)O)]$ (**4**), was obtained from the reaction of **1** with 1 equiv of DippNCO (Scheme 4).[5] The structure of **4** has been established by X-ray crystallography (Figure 4). The occurrence of the cycloaddition reactions reflects the nucleophilicity of the imido ligand in the cobalt(II) complex, which should associate with the small electronegativity of 3d metals (Pauling electronegativity: 1.36 to 1.90 for Sc−Cu, versus 3.04 for N) that renders charge polarization in their metal−nitrogen bonds. Indeed, the
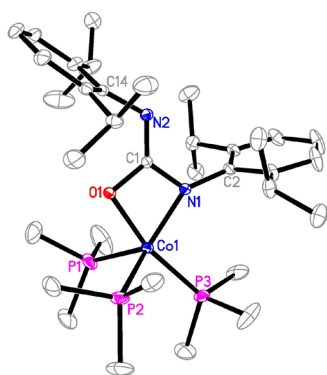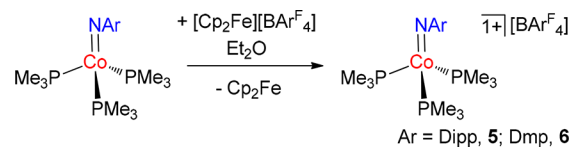
Figure 4. Molecular structure of $[(Me_3P)_3Co(\kappa^2\text{-}(Dipp)C(NDipp)\text{-}O)]$ (**4**) with 30% probability ellipsoids. Selected distances (Å) and angles (deg): Co1−N1 1.9212(17), Co1−O1 1.9437(14), Co1−C1 2.391(2), Co1−P1 2.2711(7), Co1−P2 2.2501(7), Co1−P3 2.1683(7), N1−C2 1.414(3), N1−C1 1.362(2), C1−O1 1.328(2), N2−C1 1.290(3), N2−C14 1.410(3), Co1−N1−C1 91.88(12), Co1−O1−C1 91.96(11), N1−C1−O1 107.67(17), C1−N2−C14 119.54(17).

Mulliken atomic charges on the cobalt and nitrogen atoms of **1** are +0.19 and −0.66, respectively. In contrast, the interactions of **2**, which features the sterically encumbered aryl group Dmp, with PhCHO and CS_2 led to the formation of the iminophosphine Me$_3$PNDmp in 91% and 70% NMR yields (Figure S13), respectively. While the exact causes for the differentiated reactivity of **1** and **2** are unclear, we speculate that the different steric nature of Dmp and Dipp in the two imido complexes might play a role. The attempts to isolate the cobalt-containing products in the reactions of **2** were unsuccessful.

The π^*-character of the singly occupied orbital of **1** hints at the possibility of accessing analogue cobalt(III) imido complexes upon the oxidation of the cobalt(II) species. Electrochemistry study on **1** by cyclic voltammetry disclosed the reversible one-electron redox event of $[(Me_3P)_3Co\text{-}(NDipp)]^{0/1+}$ with $E_{1/2} = -1.0$ V (vs SCE) (Figure S4). Using $[Cp_2Fe][BAr^F_4]$ ($Ar^F = 3,5\text{-di(trifluoromethyl)phenyl}$) as oxidant, the cobalt(II) imido complexes **1** and **2** were readily oxidized into the cobalt(III) imido complexes $[(Me_3P)_3Co\text{-}(NAr)][BAr^F_4]$ (Ar = Dipp, **5**; Dmp, **6**) in high yields (Scheme 5).[5] Similar to the other four-coordinate low-spin cobalt(III)

Scheme 5. One-Electron Oxidation of 1 and 2

imido complexes (**A**, **C**, and **D** in Chart 1),[3a,c,g] **5** and **6** are diamagnetic, and show well-resolved NMR spectra (^{1}H, ^{13}C, and ^{31}P NMR). A single-crystal X-ray diffraction study (Figure 5) indicated a distorted trigonal pyramidal geometry of the
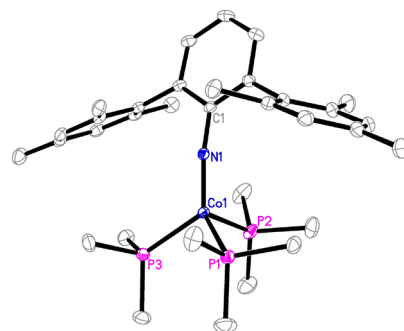
Figure 5. Structure of the cation in $[(Me_3P)_3Co(NDmp)][BAr^F_4]$ (**6**) with 30% probability ellipsoids. Selected distances (Å) and angles (deg): Co1−N1 1.6540(17), N1−C1 1.373(3), Co1−P1 2.1871(6), Co1−P2 2.1738(6), Co1−P3 2.1829(7), Co1−N1−C1 166.99(15), P1−Co1−N1 121.93(6), P2−Co1−N1 105.61(6), P3−Co1−N1 123.47(6), P1−Co1−P2 104.30(3), P1−Co1−P3 98.33(2), P2−Co1−P3 99.91(3).

cation $[(Me_3P)_3Co(NAr)]^+$ ($\tau_4 = 0.81$)[6] that was similar to those of **1**, **2**, the ruthenium imido complex $[(Me_3P)_3Ru\text{-}(NDipp)]$,[14] as well as the cobalt(III) imido complexes **A** and **C**.[3a,c] The shorter Co−N distance (1.654(2) Å) in **6** as compared with that in **2** (1.717(2) Å) is in accord with the expectation that the loss of one electron from the antibonding orbital enhances the multiple bond character of the Co−N interaction.

CONCLUSIONS

The synthesis, structure, and reactivity studies of the first low-spin cobalt(II) terminal imido complexes were achieved. The reaction of the cobalt(0) precursor $[(Me_3P)_4Co]$ with bulk organic azides serves as a facile entry to the four-coordinate cobalt(II) imido complexes $[(Me_3P)_3Co(NAr)]$ (Ar = Dipp, Dmp). X-ray diffraction studies disclosed a distorted trigonal pyramidal geometry for the CoP_3N core in the imido complexes. Spectroscopic characterization, in combination with DFT studies, indicates their low-spin nature. The cobalt(II) imido complexes could perform nitrene-transfer reaction with PMe_3 and CO, producing $Me_3PNDipp$ and DippNCNDipp, respectively. They could also undergo imido/oxo and imido/sulfido exchange reactions with PhCHO and CS_2 to give PhCHNDipp and DippNCS, respectively. In addition, the reversible one-electron redox conversion of $[(Me_3P)_3Co(NAr)]^{0/1+}$ has also been observed on the cobalt imides. The diversified reactivity of the cobalt(II) imides shows resemblance to nickel(II) imido complexes,[10c,d,15] which might be typical for late 3d transition-metal imido complexes with high d-electron counting.

EXPERIMENTAL SECTION

General Considerations. All manipulations on air- and moisture-sensitive materials were performed under an atmosphere of dry dinitrogen with the rigid exclusion of air and moisture using standard Schlenk or cannula techniques, or in a glovebox. Solvents were dried with a solvent purification system (Innovative Technology) and degassed prior to use. $[(Me_3P)_4Co]$,[16] $DippN_3$,[17a] $DmpN_3$,[17b] and $[Cp_2Fe][BAr^F_4]$[18] were synthesized according to literature procedures. All other chemicals were purchased from chemical vendors and used as received unless otherwise noted. ^1H, ^{13}C, ^{31}P, and ^{19}F NMR spectra were recorded with VARIAN 400 MHz or Agilent 400 MHz spectrometer at 400, 100, 162, and 376 MHz, respectively. All chemical shifts were reported in units of ppm with reference to the residual protons of the deuterated solvents for proton chemical shifts, the ^{13}C of deuterated solvents for carbon chemical shifts, the ^{19}F of $CFCl_3$ (external standard) for fluorine chemical shifts, and the ^{31}P of 85% phosphorous acid (external standard) for phosphine chemical shifts. HRMS-ESI spectra were recorded with an Agilent Technologies 6224 TOF LC−MS instrument. GC−MS analyses were performed on an Agilent Technologies spectrometer. Elemental analysis was performed by the Analytical Laboratory of Shanghai Institute of Organic Chemistry (CAS). Solution magnetic moments were measured at 21 °C by the method originally described by Evans with stock and experimental solutions containing a known amount of a $(CH_3)_3SiOSi(CH_3)_3$ standard.[8] Absorption spectra were recorded with a Shimadzu UV-3600 UV−vis−NIR spectrophotometer. IR spectra were recorded with Nicolet Avatar 330 FT-IR spectrophotometer or Bruker TENSOR 27 ART-FT-IR spectrophotometer. The X-band CW-EPR experiments were performed on a Bruker EMX plus spectrometer (microwave (mw) frequency 8.75−9.65 GHz) equipped with a He temperature control cryostat system (for complex 1) or a JEOL spectrometer JES-FA2000 with a liquid nitrogen cryostat system (for 2 and 4).

Caution! Organic azides are presumed to be potentially explosive. Manipulations should be handled carefully in a hood with protective equipment.

Electrochemistry. Electrochemical measurements were carried out in a glovebox under an argon atmosphere with a CHI 600D potentiostation. A glassy carbon was used as working electrode; a platinum wire was used as the auxiliary electrode, and an SCE was used as reference electrode. 0.1 M $[(n-Bu)_4N][PF_6]$ in THF was used as supporting electrolyte and was prepared in the glovebox. Under these conditions, $E_{1/2}$ = 0.55 V for the $[Cp_2Fe]^{0,+}$ couple.

X-ray Structure Determination. The structures of five compounds in Table S1 were determined. Crystals were coated with Paratone-N oil and mounted on a Bruker APEX CCD based diffractometer equipped with an Oxford low-temperature apparatus. Cell parameters were retrieved with SMART software and refined using SAINT software on all reflections. Data integration was performed with SAINT, which corrects for Lorentz polarization and decay. Absorption corrections were applied using SADABS.[19] Space groups were assigned unambiguously by analysis of symmetry and systematic absences determined by XPREP. All structures were solved and refined using SHELXTL.[20] The metal and first coordination sphere atoms were located from direct-methods E maps. Non-hydrogen atoms were found in alternating difference Fourier synthesis and least-squares refinement cycles and during the final cycles were refined anisotropically. Final crystal parameters and agreement factors are reported in Table S1.

Computational Details. Density functional theory[21] studies have been performed with the ORCA 2.8 program[22] using the B3LYP[23] method. The SVP basis set[24] was used for the N, C, and H atoms, and the TZVP basis set[25] was used for the Co and imido N atoms. The RIJCOSX approximation[26] with matching auxiliary basis sets[24,27] was employed to accelerate the calculations. The structure of 1 obtained from X-ray diffration study was used, and only positions of the hydrogen atoms are optimized. TIGHTSCF was used for SCF calculations.[28] The Mulliken spin population and Mayer bond orders of selected bonds of $[(Me_3P)_3Co(NDipp)]$ at its doublet state are shown in Figures S7 and S8, respectively. Coordinates of the calculated structure are included in the Supporting Information.

Preparation of $[(Me_3P)_3Co(NDipp)]$ (1). To a Et_2O (8 mL) solution of $[Co(PMe_3)_4]$ (660 mg, 1.82 mmol) was added a Et_2O (4 mL) solution of $DippN_3$ (739 mg, 3.64 mmol) slowly. The color of the solution changed to dark green immediately, and bubbles were released vigorously. The reaction mixture was stirred for 0.5 h at room temperature and then subjected to vacuum to remove all the volatiles. The resulting black solid was washed with *n*-pentane (2 mL × 3) and dried under vacuum to leave 1 as a brown crystalline solid (620 mg, 74%). Single crystals of 1 suitable for X-ray diffraction studies were grown by evaporation of its Et_2O solution at room temperature. ^1H NMR (400 MHz, C_6D_6, 294 K): δ (ppm) 53.34 (s, $\Delta\nu_{1/2}$ = 1520 Hz), 40.31 (s, $\Delta\nu_{1/2}$ = 1200 Hz), 22.92 (s, $\Delta\nu_{1/2}$ = 580 Hz), 4.41 (s, $\Delta\nu_{1/2}$ = 130 Hz). Anal. Calcd for $C_{21}H_{44}CoNP_3$: C 54.54, H 9.59, N 3.03. Found: C 54.44, H 9.65, N 3.16. Magnetic susceptibility (C_6D_6, 294 K): μ_{eff} = 1.9(1) μ_B. Absorption spectrum (in THF): λ_{max}, nm (ε, M^{-1} cm^{-1}) 300 (12 000), 320 (15 600), 380 (4900), 530 (750), 710 (1250), 960 (440). IR (KBr, cm^{-1}): ν = 2958 (m), 2896 (m), 2864 (w), 1576 (m), 1458 (m), 1433 (m), 1418 (m), 1400 (m), 1363 (m), 1300 (s), 1283 (s), 1258 (m), 1164 (s), 1132 (m), 946 (s), 871 (m), 862 (m), 741 (m), 714 (m), 656 (w). After the black solid of 1 was separated, the mother liquor of the *n*-pentane solution was collected. Slow evaporation of the *n*-pentane solution at room temperature afforded light yellow crystals that were collected and washed with drops of *n*-hexane, giving the iminophosphine $Me_3PNDipp$ as light yellow crystals (324 mg, 71%). ^1H NMR (400 MHz, C_6D_6, 294 K): δ (ppm) 7.27−7.20 (m, 2H), 7.07 (td, J = 7.6, 2.5 Hz, 1H), 3.59 (septet, J = 6.9 Hz, 2H), 1.34 (d, J = 6.9 Hz, 12H), 0.93 (d, $J_{P−H}$ = 12.0 Hz, 9H). ^{13}C NMR (100 MHz, C_6D_6, 294 K): δ (ppm) 145.8 (d, $J_{P−C}$ = 2.9 Hz), 142.4 (d, $J_{P−C}$ = 7.3 Hz), 122.9 (d, $J_{P−C}$ = 3.2 Hz), 119.6 (d, $J_{P−C}$ = 4.0 Hz), 28.7, 24.2, 17.7 (d, $J_{P−C}$ = 69 Hz). ^{31}P NMR (162 MHz, C_6D_6, 294 K): δ (ppm) −8.23. HRMS (ESI) calcd for $C_{15}H_{27}NP$ $[M + H]^+$: 252.1881. Found $[M + H]^+$: 252.1875. IR (powder, cm^{-1}): ν = 3057 (w), 2956 (s), 2872 (w), 1441 (s), 1358 (s), 1292 (m), 1069 (w), 933 (s), 849 (w), 768 (w), 732 (w).

Preparation of $[(Me_3P)_3Co(NDmp)]$ (2). To a Et_2O (5 mL) solution of $[Co(PMe_3)_4]$ (182 mg, 0.50 mmol) was slowly added $DmpN_3$ (180 mg, 0.50 mmol). The color of the solution changed to brown immediately, and bubbles were released vigorously. The reaction mixture was stirred for 2 h at room temperature and then subjected to vacuum to remove all the volatiles. The resulting black solid was washed with *n*-pentane (2 mL × 3) and dried under vacuum to leave 2 as a brown solid (250 mg, 81%). Single crystals of 2 suitable for X-ray diffraction studies were grown by evaporation of its Et_2O solution at room temperature. ^1H NMR (400 MHz, C_6D_6, 294 K): δ (ppm) 24.88

(s, $\Delta\nu_{1/2}$ = 1940 Hz), 14.82 (s, $\Delta\nu_{1/2}$ = 260 Hz), 6.33 (s, $\Delta\nu_{1/2}$ = 120 Hz), 5.72 (s, $\Delta\nu_{1/2}$ = 190 Hz). Anal. Calcd for $C_{33}H_{52}CoNP_3$: C 64.49, H 8.53, N 2.28. Found: C 64.43, H 8.42, N 2.23. Magnetic susceptibility (C_6D_6, 294 K): μ_{eff} = 2.1(1) μ_B. Absorption spectrum (in THF): λ_{max}, nm (ε, M^{-1} cm^{-1}) 300 (13 500), 330 (17 300), 380 (6400), 440 (2700), 540 (1240), 710 (1000), 990 (330). IR (KBr, cm^{-1}): ν = 2956 (s), 2912 (s), 2854 (m), 1609 (w), 1569 (w), 1451 (s), 1339 (m), 1297 (m), 1167 (s), 1104 (m), 937 (s), 851 (s), 751 (m).

Reaction of 1 with Me₃P. To a C_6D_6 (0.4 mL) solution of [(Me₃P)₃Co(NDipp)] (1, 14 mg, 0.03 mmol) in a J. Young NMR tube was added excess Me₃P (23 mg, 0.30 mmol), and 1,3,5-trimethoxybenzene (5.5 mg, 0.033 mmol, as internal standard). The reaction mixture was standing at room temperature and monitored by ^1H NMR spectroscopy; during the course of the reaction, the color of the solution changed to brown gradually. After 2 h, ^1H NMR spectrum analysis indicated the clean formation of [(Me₃P)₄Co] and the formation of the iminophosphine Me₃PNDipp in 80% NMR yield (Figure S9). For [(Me₃P)₄Co], ^1H NMR (400 MHz, C_6D_6, 294 K): δ (ppm) 33.72 (s, $\Delta\nu_{1/2}$ = 170 Hz). The ^1H NMR spectrum is identical to that reported in the literature.[16]

Reaction of DippN₃ with Me₃P. To a C_6D_6 (0.4 mL) solution of DippN₃ (10 mg, 0.05 mmol) in a J. Young NMR tube was added Me₃P (5.8 mg, 0.08 mmol) at room temperature. The color of the solution remained light yellow, and bubbles were released slowly. After 20 min at room temperature, ^1H NMR spectrum analysis indicated the clean formation of iminophosphine Me₃PNDipp (Figure S11). Scaled-up reaction in toluene (8 mL) by using DippN₃ (407 mg, 2.0 mmol) and Me₃P (228 mg, 3.0 mmol) at room temperature for 0.5 h gave the iminophosphine Me₃PNDipp (483 mg, 96% yield) as a light yellow solid.

Reaction of DmpN₃ with Me₃P. To a C_6D_6 (0.4 mL) solution of DmpN₃ (18 mg, 0.05 mmol) in a J. Young NMR tube was added Me₃P (5.8 mg, 0.08 mmol) at room temperature. The color of the solution remained light yellow, and bubbles were released slowly. After 20 min at room temperature, ^1H NMR spectrum analysis indicated the clean formation of iminophosphine Me₃PNDmp (Figure S12). Scaled-up reaction in toluene (5 mL) solution by using DmpN₃ (142 mg, 0.4 mmol) and Me₃P (46 mg, 0.6 mmol) at room temperature for 0.5 h gave the iminophosphine Me₃PNDmp as a light yellow solid (152 mg, 94%). ^1H NMR (400 MHz, C_6D_6, 294 K): δ (ppm) 7.14 (m, 2H), 6.98 (td, J = 7.2, 2.4 Hz, 1H), 6.92 (s, 4H), 2.32 (s, 12H), 2.26 (s, 6H), 0.40 (d, J_{P-H} = 12.5 Hz, 9H). ^{13}C NMR (100 MHz, C_6D_6, 294 K): δ (ppm) 146.8, 140.8, 137.1, 136.6 (d, J_{P-C} = 6.9 Hz), 135.2, 129.2, 128.1, 118.6 (d, J_{P-C} = 3.0 Hz), 21.3, 21.1, 17.5 (d, J_{P-C} = 69 Hz). ^{31}P NMR (162 MHz, C_6D_6, 294 K): δ (ppm) −9.34. HRMS (ESI) calcd for $C_{27}H_{36}NP$ $[M + H]^+$: 404.2507. Found $[M + H]^+$: 404.2503. IR (powder, cm^{-1}): ν = 2986 (w), 2945 (w), 2912 (w), 2852 (w), 1429 (s), 1335 (m), 1283 (w), 1100 (m), 933 (s), 847 (m), 762 (m), 731 (w).

Reaction of 1 with (E)-MeO₂CCH=CHCO₂Me. To a C_6D_6 (0.4 mL) solution of [(Me₃P)Co(NDipp)] (1, 14 mg, 0.03 mmol) in a J. Young NMR tube was added (E)-MeO₂CCH=CHCO₂Me (4.3 mg, 0.03 mmol). The reaction mixture was monitored by ^1H NMR spectroscopy at room temperature; during the course of the reaction the color of the solution changed to brown gradually. After 1 h, 1 was consumed completely, and then 1,3,5-trimethoxybenzene (4.7 mg, 0.028 mmol) was added as the internal standard. ^1H NMR spectrum analysis indicated the formation of the iminophosphine Me₃PNDipp (88% NMR yield) and [(Me₃P)₃Co(η^2-(E)-MeCO₂CH=CHCO₂Me)] (3).

Isolation of [(Me₃P)₃Co(η²-(E)-MeCO₂CH=CHCO₂Me)] (3). To a toluene (8 mL) solution of [(Me₃P)₃Co(NDipp)] (1, 139 mg, 0.30 mmol) was added (E)-MeO₂CCH=CHCO₂Me (43 mg, 0.30 mmol). The reaction mixture was stirred for 1 h at room temperature; during the course of the reaction the color of the solution changed to brown gradually. Then the volatiles were removed under vacuum to yield a brown solid that was then washed with n-hexane (3 mL × 3) first, then extracted with toluene (3 mL), and filtered. Standing the toluene solution at −30 °C overnight gave 3 as brown crystals (52 mg, 40%,

based on cobalt). ^1H NMR (400 MHz, C_6D_6, 294 K): δ (ppm) 35.84 (s, $\Delta\nu_{1/2}$ = 2390 Hz), −1.15 (s, $\Delta\nu_{1/2}$ = 130 Hz). Anal. Calcd for $C_{15}H_{35}CoO_4P_3$: C 41.77, H 8.18. Found: C 41.79, H 8.36. Magnetic susceptibility (C_6D_6, 294 K): μ_{eff} = 2.1(1) μ_B. Absorption spectrum (in THF): λ_{max}, nm (ε, M^{-1} cm^{-1}) 300 (14 300), 400 (1830), 920 (80), 1160 (100). IR (KBr, cm^{-1}): ν = 2963 (m), 2981 (m), 2908 (m), 2807 (w), 1723 (s), 1671 (s), 1659 (s), 1591 (s), 1440 (s), 1302 (s), 1283 (s), 1253 (m), 1233 (m), 1170 (s), 1043 (m), 1013 (w), 991 (m), 946 (s), 871 (m), 862 (m), 745 (m), 673 (w), 660 (w).

Reaction of 1 with CO. The toluene (5 mL) solution of [(Me₃P)₃Co(NDipp)] (1, 93 mg, 0.20 mmol) in a 25 mL flask was quickly frozen with liquid N_2 and subjected to vacuum to remove the N_2 atmosphere in the flask. Then CO was introduced to the mixture via a CO balloon (1 atm). The reaction mixture was allowed to warm to room temperature. The color of the solution changed from green to orange immediately. After 10 min, the volatiles were removed under vacuum to yield brown solid that was then extracted with n-pentane (3 mL × 2) and filtered. Then the filtrate was exposed to air and wet n-hexane (2 mL) was added to quench the cobalt species. After flash column chromatography separation (silica gel, n-hexane as elute), DippNCNDipp was obtained as a light yellow oil (47 mg, 86%). ^1H NMR (400 MHz, C_6D_6, 294 K): δ (ppm) 7.05 (s, 6H), 3.66 (septet, J = 6.9 Hz, 4H), 1.24 (d, J = 6.9 Hz, 24H). The ^1H NMR spectrum is identical to that reported in the literature.[11c]

Reaction of 1 with PhCHO. To a toluene (2 mL) solution of [(Me₃P)₃Co(NDipp)] (1, 92 mg, 0.20 mmol) was added PhCHO (24 mg, 0.23 mmol). The reaction mixture was stirred for 2 h at room temperature; during the course of the reaction the color of the solution changed to brown gradually. Then the solution was exposed to air and wet n-hexane (2 mL) was added to quench the cobalt species. After column chromatography separation (silica gel, 20:1 n-hexane/CH_2Cl_2), DippNCHPh was obtained as a yellow oil (38 mg, 72%). ^1H NMR (400 MHz, $CDCl_3$, 294 K): δ (ppm) 8.24 (s, 1H), 8.01−7.89 (m, 2H), 7.62−7.49 (m, 3H), 7.24−7.11 (m, 3H), 3.02 (septet, J = 6.9 Hz, 2H), 1.21 (d, J = 6.9 Hz, 12H). GC−MS: m/z = 265.1 ($[M]^+$). The ^1H NMR spectrum is identical to that reported in the literature.[29]

Reaction of 1 with CS₂. To a Et_2O (2 mL) solution of CS₂ (23 mg, 0.30 mmol) was slowly added a Et_2O (2 mL) solution of [(Me₃P)₃Co(NDipp)] (1, 46 mg, 0.10 mmol). The reaction mixture was stirred for 30 min at room temperature; during the course of the reaction the color of the solution changed to brown gradually. The volatiles were removed under vacuum to yield a brown solid that was then extracted with n-hexane (3 mL × 2) and filtered through Celite. The filtrate was exposed to air and wet n-hexane (2 mL) was added to quench the cobalt species, and then the reaction mixture was filtered through Celite again. Removal of the volatiles under vacuum afforded DippNCS as a light yellow solid (20 mg, 90%). ^1H NMR (400 MHz, $CDCl_3$, 294 K): δ (ppm) 7.24 (t, J = 7.9 Hz 1H), 7.14 (d, J = 7.6 Hz, 2H), 3.26 (septet, J = 6.9 Hz, 2H), 1.28 (d, J = 6.9 Hz, 12H). GC−MS: m/z = 219.1 ($[M]^+$). The ^1H NMR spectrum is identical to that reported in the literature.[30]

Reaction of 1 with DippNCO. To a toluene (8 mL) solution of [(Me₃P)₃Co(NDipp)] (1, 159 mg, 0.34 mmol) was added DippNCO (77 mg, 0.38 mmol). The reaction mixture was stirred for 3 h at room temperature; during the course of the reaction the color of the solution changed to brown gradually. The volatiles were removed under vacuum to yield a brown solid that was washed with n-hexane (3 mL × 3) first, then extracted with THF (3 mL), and filtered. Slow evaporation of the THF solution at room temperature gave [(Me₃P)₃Co(κ^2-N(Dipp)C(NDipp)O)] (4) as brown crystals (114 mg, 50%). ^1H NMR (400 MHz, C_6D_6, 294 K): δ (ppm) 14.74 (s, $\Delta\nu_{1/2}$ = 430 Hz), 13.64 (s, $\Delta\nu_{1/2}$ = 400 Hz), 8.06 (s, $\Delta\nu_{1/2}$ = 40 Hz), 5.95 (s, $\Delta\nu_{1/2}$ = 35 Hz), 4.16 (s, $\Delta\nu_{1/2}$ = 380 Hz), 1.87 (s, $\Delta\nu_{1/2}$ = 60 Hz), 1.00 (s, $\Delta\nu_{1/2}$ = 150 Hz). Anal. Calcd for $C_{34}H_{61}CoN_2OP_3$: C 61.34, H 9.24, N 4.21. Found: C 61.34, H 8.92, N 3.73. Magnetic susceptibility (C_6D_6, 294 K): μ_{eff} = 2.0(1) μ_B. Absorption spectrum (in THF): λ_{max}, nm (ε, M^{-1} cm^{-1}) 280 (10 000), 450 (2050), 650 (120), 840 (350), 1100 (130). IR (KBr, cm^{-1}): ν = 2961 (m), 2900 (m), 2866 (m), 1683 (m), 1594 (w), 1549 (s), 1466 (w), 1433 (m), 1337

(w), 1307 (w), 1294 (m), 1246 (w), 1152 (m), 940 (s), 907 (w), 776 (w), 749 (w).

Reactions of [(Me₃P)Co(NDmp)] (2) with PhCHO and CS₂. To C_6D_6 (0.4 mL) solutions of $[(Me_3P)_3Co(NDmp)]$ (2) (12.3 mg, 0.02 mmol) in J. Young NMR tube were added equimolar amounts of PhCHO and CS_2, respectively. Then, 1,3,5-trimethoxybenzene was added as internal standard, and the reactions were monitored by ¹H NMR spectroscopy at room temperature until there was complete consumption of **2**. ¹H NMR spectrum analyses (Figure S13) show the clean formation of the iminophosphine Me₃PNDmp in 91% and 70% NMR yields, respectively.

Preparation of [(Me₃P)₃Co(NDipp)][BArᶠ₄] (5). To a Et_2O (8 mL) solution of $[(Me_3P)_3Co(NDipp)]$ (1, 153 mg, 0.33 mmol) was slowly added $[Cp_2Fe][BAr^F_4]$ (346 mg, 0.33 mmol). The color of the solution changed to brownish red immediately. The reaction mixture was stirred for 3 h at room temperature and then subjected to vacuum to remove all the volatiles. The resulting red solid was washed with *n*-hexane (3 mL × 3) first, then extracted with Et_2O (5 mL), and filtered. The dark red crystalline solid of **5** (350 mg, 87%) was obtained by slow diffusion of *n*-hexane (10 mL) to its Et_2O solution at −30 °C. ¹H NMR (400 MHz, d_8-THF, 294 K): δ (ppm) 7.80 (br, 8H), 7.71 (t, *J* = 7.7 Hz, 1H), 7.58 (br, 4H), 6.79 (d, *J* = 7.8 Hz, 2H), 3.40 (septet, *J* = 6.9 Hz, 2H), 1.74 (d, J_{P-H} = 8.9 Hz, 27H), 1.16 (d, *J* = 6.9 Hz, 12H). ¹³C NMR (100 MHz, d_8-THF, 294 K): δ (ppm) 162.6 (q, *J* = 49.6 Hz, *C*-B), 141.0 (d, *J* = 5.1 Hz), 135.4, 129.8 (q, *J* = 31.9 Hz, *C*-CF₃), 127.6, 125.7, 125.3 (q, *J* = 270.8 Hz, CF₃), 118.01, 29.1, 22.6, 20.0 (d, *J* = 27.0 Hz). ¹⁹F NMR (376 MHz, d_8-THF, 294 K): δ (ppm) −61.47 (s). ³¹P NMR (162 MHz, d_8-THF, 294 K): δ (ppm) 12.04 (br). Anal. Calcd for $C_{53}H_{56}BCoF_{24}NP_3$: C 48.02, H 4.26, N 1.06. Found: C 47.58, H 4.31, N 0.86. Absorption spectrum (in THF): λ_{max}, nm (ε, M^{-1} cm^{-1}) 310 (10 500), 420 (3000), 550 (1800), 660 (470), 950 (72). IR (KBr, cm^{-1}): ν = 2971 (w), 1611 (w), 1464 (w), 1427 (w), 1355 (s), 1278 (s), 1166 (s), 1128 (s), 940 (m), 888 (m), 839 (m), 716 (m), 682 (m), 669 (m).

Preparation of [(Me₃P)₃Co(NDmp)][BArᶠ₄] (6). To a Et_2O (8 mL) solution of $[(Me_3P)_3Co(NDmp)]$ (2, 123 mg, 0.20 mmol) was slowly added $[Cp_2Fe][BAr^F_4]$ (210 mg, 0.20 mmol). The color of the solution changed to brownish red immediately. The reaction mixture was stirred for 3 h at room temperature and then subjected to vacuum to remove all the volatiles. The resulting red solid was washed with *n*-hexane (3 mL × 3) first, then extracted with Et_2O (5 mL), and filtered. Dark red crystals of **6** (183 mg, 62%) were obtained by slow evaporation of its Et_2O solution at room temperature. ¹H NMR (400 MHz, d_8-THF, 294 K): δ (ppm) 7.79 (br, 8H), 7.58 (br, 4H), 6.96 (s, 4H), 6.59 (d, *J* = 7.6 Hz, 2H), 2.32 (s, 6H), 2.03 (s, 12H), 1.30 (d, *J* = 10.1 Hz, 27H). ¹³C NMR (100 MHz, d_8-THF, 294 K): δ (ppm) 162.6 (q, *J* = 48.8 Hz, *C*-B), 139.6, 138.0, 135.4 (two peaks included), 133.5 (d, *J* = 6.3 Hz), 133.2, 129.9 (q, *J* = 28.4 Hz, *C*-CF₃), 129.6, 127.0, 125.3 (q, *J* = 270.9 Hz, CF₃), 118.0, 21.2, 20.9, 20.3 (d, *J* = 27.5 Hz) (one peak was not observed due to overlapping). ¹⁹F NMR (376 MHz, d_8-THF, 294 K): δ (ppm) −63.39 (s). ³¹P NMR (162 MHz, d_8-THF, 294 K): δ (ppm) 16.09 (br). Anal. Calcd for $C_{63}H_{58}BCoF_{24}NP_3$: C 52.83, H 4.37, N 0.95. Found: C 52.87, H 4.27, N 0.71. Absorption spectrum (in THF): λ_{max}, nm (ε, M^{-1} cm^{-1}) 310 (18 800), 420 (7100), 550 (4100), 680 (790). IR (KBr, cm^{-1}): ν = 2976 (w), 1611 (w), 1425 (w), 1355 (s), 1285 (s), 1170 (s), 1126 (s), 961 (m), 940(w), 888(m), 839 (w), 715(w), 682 (m), 669 (m).

■ ASSOCIATED CONTENT

ⓢ Supporting Information

The Supporting Information is available free of charge on the ACS Publications website at DOI: 10.1021/acs.inorgchem.7b00941.

> Table of crystal data, molecular structures, absorption spectra, NMR spectra, EPR spectra, cyclic voltammogram, Mulliken spin populations and bond orders of the calculated structure, and Cartesian coordinates of the optimized structure (PDF)

■ AUTHOR INFORMATION

Corresponding Author

*E-mail: deng@sioc.ac.cn.

ORCID Ⓞ

Yang Liu: 0000-0002-2486-8520

Jingzhen Du: 0000-0003-4037-9281

Liang Deng: 0000-0002-0964-9426

Notes

The authors declare no competing financial interest.

■ ACKNOWLEDGMENTS

■ REFERENCES

(1) (a) Berry, J. F. Terminal nitrido and imido complexes of the late transition metals. *Comments Inorg. Chem.* **2009**, *30*, 28−66. (b) Saouma, C. T.; Peters, J. C. M≡E and M = E complexes of iron and cobalt that emphasize three-fold symmetry (E≡O, N, NR). *Coord. Chem. Rev.* **2011**, *255*, 920−937. (c) Ray, K.; Heims, F.; Pfaff, F. F. Terminal oxo and imido transition-metal complexes of groups 9−11. *Eur. J. Inorg. Chem.* **2013**, *2013*, 3784−3807. (d) Shin, K.; Kim, H.; Chang, S. Transition-metal-catalyzed C−N bond forming reactions using organic azides as the nitrogen source: a Journey for the mild and versatile C−H amination. *Acc. Chem. Res.* **2015**, *48*, 1040−1052. (e) Cundari, T. R. Computational studies of transition metal-main group multiple bonding. *Chem. Rev.* **2000**, *100*, 807−818.

(2) (a) Lyaskovskyy, V.; Suarez, A. I. O.; Lu, H.; Jiang, H.; Zhang, X. P.; de Bruin, B. Mechanism of cobalt(II) porphyrin-catalyzed C-H amination with organic azides: radical nature and H-atom abstraction ability of the key cobalt(III)nitrene intermediates. *J. Am. Chem. Soc.* **2011**, *133*, 12264−12273. (b) Jin, L.-M.; Xu, X.; Lu, H.; Cui, X.; Wojtas, L.; Zhang, X. P. Effective synthesis of chiral N-fluoroaryl aziridines through enantioselective aziridination of alkenes with fluoroaryl azides. *Angew. Chem., Int. Ed.* **2013**, *52*, 5309−5313. (c) Goswami, M.; Lyaskovskyy, V.; Domingos, S. R.; Buma, W. J.; Woutersen, S.; Troeppner, O.; Ivanović-Burmazović, I.; Lu, H.; Cui, X.; Zhang, X. P.; Reijerse, E. J.; DeBeer, S.; van Schooneveld, M. M.; Pfaff, F. F.; Ray, K.; de Bruin, B. Characterization of porphyrin-Co(III)-'nitrene radical' species relevant in catalytic nitrene transfer reactions. *J. Am. Chem. Soc.* **2015**, *137*, 5468−5479. (d) Cundari, T. R. Transition metal imido complexes. *J. Am. Chem. Soc.* **1992**, *114*, 7879−7888. (e) Wasbotten, I. H.; Ghosh, A. Spin-state energetics and spin-crossover behavior of pseudotetrahedral cobalt(III)-imido complexes. The role of the tripodal supporting ligand. *Inorg. Chem.* **2007**, *46*, 7890−7898. (f) Conradie, J.; Ghosh, A. Electronic structure of trigonal-planar transition-metal-imido complexes: spin-state energetics, spin-density profiles, and the remarkable performance of the OLYP functional. *J. Chem. Theory Comput.* **2007**, *3*, 689−702. (g) Hu, L.; Chen, H. What factors control the reactivity of cobalt−imido complexes in C−H bond activation via hydrogen abstraction? *ACS Catal.* **2017**, *7*, 285−292.

(3) (a) Jenkins, D. M.; Betley, T. A.; Peters, J. C. Oxidative group transfer to Co(I) affords a terminal Co(III) imido complex. *J. Am. Chem. Soc.* **2002**, *124*, 11238−11239. (b) Betley, T. A.; Peters, J. C. Dinitrogen chemistry from trigonally coordinated iron and cobalt platforms. *J. Am. Chem. Soc.* **2003**, *125*, 10782−10783. (c) Hu, X.; Meyer, K. Terminal cobalt(III) imido complexes supported by tris(carbene) ligands: imido insertion into the cobalt-carbene bond. *J. Am. Chem. Soc.* **2004**, *126*, 16322−16323. (d) Dai, X.; Kapoor, P.; Warren, T. H. [Me$_2$NN]Co(η^6-toluene): O=O, N=N, and O=N bond cleavage provides β-diketiminato cobalt μ-oxo and imido complexes. *J. Am. Chem. Soc.* **2004**, *126*, 4798−4799. (e) Shay, D. T.; Yap, G. P. A.; Zakharov, L. N.; Rheingold, A. L.; Theopold, K. H. *Angew. Chem., Int. Ed.* **2005**, *44*, 1508−1510. (f) Mehn, M. P.; Brown, S. D.; Jenkins, D. M.; Peters, J. C.; Que, L., Jr. Vibrational spectroscopy and analysis of pseudo-tetrahedral complexes with metal imido bonds. *Inorg. Chem.* **2006**, *45*, 7417−7427. (g) Cowley, R. E.; Bontchev, R. P.; Sorrell, J.; Sarracino, O.; Feng, Y.; Wang, H.; Smith, J. M. Formation of a cobalt(III) imido from a cobalt(II) amido complex. Evidence for proton-coupled electron transfer. *J. Am. Chem. Soc.* **2007**, *129*, 2424−2425. (h) Jones, C.; Schulten, C.; Rose, R. P.; Stasch, A.; Aldridge, S.; Woodul, W. D.; Murray, K. S.; Moubaraki, B.; Brynda, M.; Macchia, G. L.; Gagliardi, L. Amidinato- and guanidinato-cobalt(I) complexes: characterization of exceptionally short Co-Co interactions. *Angew. Chem., Int. Ed.* **2009**, *48*, 7406−7410. (i) King, E. R.; Sazama, G. T.; Betley, T. A. Co(III) imidos exhibiting spin crossover and C-H bond activation. *J. Am. Chem. Soc.* **2012**, *134*, 17858−17861. (j) Wu, B.; Hernández Sánchez, R.; Bezpalko, M. W.; Foxman, B. M.; Thomas, C. M. Formation of heterobimetallic zirconium/cobalt diimido complexes via a four-electron transformation. *Inorg. Chem.* **2014**, *53*, 10021−10023.

(4) (a) Du, J.; Wang, L.; Xie, M.; Deng, L. A two-coordinate cobalt(II) imido complex with NHC ligation: synthesis, structure, and reactivity. *Angew. Chem., Int. Ed.* **2015**, *54*, 12640−12644. (b) Yao, X.-N.; Du, J.-Z.; Zhang, Y.-Q.; Leng, X.-B.; Yang, M.-W.; Jiang, S.-D.; Wang, Z.-X.; Ouyang, Z.-W.; Deng, L.; Wang, B.-W.; Gao, S. Two-coordinate Co(II) imido complexes as outstanding single-molecule magnets. *J. Am. Chem. Soc.* **2017**, *139*, 373−380. (c) Zhang, L.; Liu, Y.-S.; Deng, L. Three coordinate cobalt(IV) and cobalt(V) imido complexes with N-heterocyclic carbene ligation: synthesis, structure, and their distinct reactivity in C-H bond amination. *J. Am. Chem. Soc.* **2014**, *136*, 15525−15528.

(5) Please see the Experimental Section and Supporting Information for detailed information.

(6) Yang, L.; Powell, D. R.; Houser, R. P. Structural variation in copper(I) complexes with pyridylmethylamide ligands: structural analysis with a new four-coordinate geometry index, τ_4. *Dalton Trans.* **2007**, 955−964.

(7) Jenkins, D. M.; Di Bilio, A. J.; Allen, M. J.; Betley, T. A.; Peters, J. C. Elucidation of a low spin cobalt(II) system in a distorted tetrahedral geometry. *J. Am. Chem. Soc.* **2002**, *124*, 15336−15350.

(8) (a) Evans, D. F. The determination of the paramagnetic susceptibility of substances in solution by nuclear magnetic resonance. *J. Chem. Soc.* **1959**, 2003−2005. (b) Sur, S. K. Measurement of magnetic susceptibility and magnetic moment of paramagnetic molecules in solution by high-field fourier transform NMR spectroscopy. *J. Magn. Reson.* **1989**, *82*, 169−173.

(9) For examples, see: (a) Johnson, J. B.; Rovis, T. More than bystanders: the effect of olefins on transition-metal-catalyzed cross-coupling reactions. *Angew. Chem., Int. Ed.* **2008**, *47*, 840−871. (b) Liu, Y.; Xiao, J.; Wang, L.; Song, Y.; Deng, L. Carbon−Carbon bond formation reactivity of a four-coordinate NHC-supported iron(II) phenyl compound. *Organometallics* **2015**, *34*, 599−605.

(10) (a) Nugent, W. A.; Mayer, J. M. *Metal−Ligand Multiple Bonds: The Chemistry of Transition Metal Complexes Containing Oxo, Nitrido, Imido, Alkylidene Ligands*; Wiley: New York, 1988. (b) Eikey, R. A.; Abu-Omar, M. M. Nitrido and imido transition metal complexes of Groups 6−8. *Coord. Chem. Rev.* **2003**, *243*, 83−124. (c) Mindiola, D. J.; Hillhouse, G. L. Isocyanate and carbodiimide synthesis by nitrene-group-transfer from a nickel(II) imido complex. *Chem. Commun.* **2002**,

1840−1841. (d) Kogut, E.; Wiencko, H. L.; Zhang, L.; Cordeau, D. E.; Warren, T. H. A Terminal Ni(III)-imide with diverse reactivity pathways. *J. Am. Chem. Soc.* **2005**, *127*, 11248−11249. (e) Cowley, R. E.; Eckert, N. A.; Elhaïk, J.; Holland, P. L. Catalytic nitrene transfer from an imidoiron(III) complex to form carbodiimides and isocyanates. *Chem. Commun.* **2009**, 1760−1762. (f) Geer, A. M.; Tejel, C.; López, J. A.; Ciriano, M. A. Terminal imido Rhodium complexes. *Angew. Chem., Int. Ed.* **2014**, *53*, 5614−5618. (g) Wang, L.; Hu, L.; Zhang, H.; Chen, H.; Deng, L. Three-coordinate iron(IV) bisimido complexes with aminocarbene ligation: synthesis, structure, and reactivity. *J. Am. Chem. Soc.* **2015**, *137*, 14196−14207.

(11) For examples of formation carbodiimide via [2π + 2π] and retro-[2π + 2π]-addition of early transition-metal imido complexes with isocyanates, please see: (a) Walsh, P. J.; Hollander, F. J.; Bergman, R. G. Monomeric and dimeric zirconocene imido compounds: synthesis, structure, and reactivity. *Organometallics* **1993**, *12*, 3705−3723. (b) Birdwhistell, K. R.; Boucher, T.; Ensminger, M.; Harris, S.; Johnson, M.; Toporek, S. Catalysis of phenyl isocyanate condensation to *N,N′*-diphenylcarbodiimide via vanadium oxo and imido complexes. *Organometallics* **1993**, *12*, 1023−1025. (c) Kilgore, U. J.; Basuli, F.; Huffman, J. C.; Mindiola, D. J. Aryl isocyanate, carbodiimide, and isocyanide prepared from carbon dioxide. A metathetical group-transfer tale involving a titanium-imide zwitterion. *Inorg. Chem.* **2006**, *45*, 487−489. (d) Dunn, S. C.; Hazari, N.; Cowley, A. R.; Green, J. C.; Mountford, P. Synthesis and reactions of group 4 imido complexes supported by cyclooctatetraene ligands. *Organometallics* **2006**, *25*, 1755−1700. (e) Darwish, W.; Seikel, E.; Käsmarker, R.; Harms, K.; Sundermeyer, J. Synthesis and X-ray crystal structures of imido and ureato derivatives of titanium(IV) phthalocyanine and their application in the catalytic formation of carbodiimides by metathesis from isocyanates. *Dalton Trans.* **2011**, *40*, 1787−1794.

(12) (a) Ulrich, H.; Tucker, B.; Sayigh, A. A. R. Metal carbonyls as catalysts in the conversion of isocyanates to carbodiimides. *Tetrahedron Lett.* **1967**, *8*, 1731−1733. (b) Rahman, A. K. F.; Nicholas, K. M. Catalytic conversion of isocyanates to carbodiimides by cyclopentadienyl manganese tricarbonyl and cyclopentadienyl iron dicarbonyl dimer. *Tetrahedron Lett.* **2007**, *48*, 6002−6004.

(13) For examples of formation imine and isothiocyanate via [2π + 2π] and retro-[2π + 2π]-addition of early transition-metal imido complexes with carbonyl compounds and CS$_2$, please see ref 11d and: (a) Lee, S. Y.; Bergman, R. G. Generation of oxozirconocene complexes from the reaction of Cp$_2$(THF)Zr=N-*t*-Bu with organic and metal carbonyl functionalities: apparently divergent behavior of transient [Cp$_2$Zr=O]. *J. Am. Chem. Soc.* **1996**, *118*, 6396−6406. (b) Zuckerman, R. L.; Bergman, R. G. Structural factors that influence the course of overall [2 + 2] cycloaddition reactions between imidozirconocene complexes and heterocumulenes. *Organometallics* **2000**, *19*, 4795−4809.

(14) Singh, A. K.; Levine, B. G.; Staples, R. J.; Odom, A. L. A 4-coordinate Ru(II) imido: unusual geometry, synthesis, and reactivity. *Chem. Commun.* **2013**, *49*, 10799−10801.

(15) For examples, see: (a) Mindiola, D. J.; Hillhouse, G. L. Terminal amido and imido complexes of three-coordinate nickel. *J. Am. Chem. Soc.* **2001**, *123*, 4623−4624. (b) Mindiola, D. J.; Waterman, R.; Iluc, V. M.; Cundari, T. R.; Hillhouse, G. L. Carbon−Hydrogen bond activation, C−N bond coupling, and cycloaddition reactivity of a three-coordinate nickel complex featuring a terminal imido ligand. *Inorg. Chem.* **2014**, *53*, 13227−13238.

(16) Klein, H.-F.; Karsch, H. H. Methyltetrakis(trimethy1phosphin)-kobalt und seine derivate. *Chem. Ber.* **1975**, *108*, 944−955.

(17) (a) Guisado-Barrios, G.; Bouffard, J.; Donnadieu, B.; Bertrand, G. Crystalline 1*H*-1,2,3-triazol-5-ylidenes: new stable mesoionic carbenes (MICs). *Angew. Chem., Int. Ed.* **2010**, *49*, 4759−4762. (b) Gavenonis, J.; Tilley, T. D. Tantalum alkyl and silyl complexes of the bulky (terphenyl)imido ligand [2,6-(2,4,6-Me$_3$C$_6$H$_2$)$_2$C$_6$H$_3$N =]$^{2-}$([Ar*N =]$^{2-}$). Generation and reactivity of [(Ar*N =)(Ar*NH)-Ta(H)(OSO$_2$CF$_3$)], which reversibly transfers hydride to an aromatic ring of the arylamide ligand. *Organometallics* **2002**, *21*, 5549−5563.

(18) Chávez, I.; Alvarez-Carena, A.; Molins, E.; Roig, A.; Maniukiewicz, W.; Arancibia, A.; Arancibia, V.; Brand, H.; Manríquez, J. M. Selective oxidants for organometallic compounds containing a stabilising anion of highly reactive cations: (3,5-$(CF_3)_2C_6H_3)_4B^-$)Cp_2Fe^+ and (3,5$(CF_3)_2C_6H_3)_4B^-$)$Cp*_2Fe^+$. *J. Organomet. Chem.* **2000**, *601*, 126−132.

(19) Sheldrick, G. M. *SADABS: Program for Empirical Absorption Correction of Area Detector Data*; University of Göttingen: Germany, 1996.

(20) Sheldrick, G. M. *SHELXTL 5.10 for Windows NT: Structure Determination Software Programs*; Bruker Analytical X-ray Systems, Inc.: Madison, WI, 1997.

(21) (a) Hohenberg, P.; Kohn, W. Inhomogeneous electron gas. *Phys. Rev.* **1964**, *136*, B864−B871. (b) Kohn, W.; Sham, L. J. Self-consistent equations including exchange and correlation effects. *Phys. Rev.* **1965**, *140*, A1133−A1138.

(22) Neese, F. *ORCA: An ab Initio, Density Functional and Semiempirical Program Package (v. 2.8)*; Universität Bonn, 2011.

(23) (a) Becke, A. D. Density-functional thermochemistry. III. The role of exact exchange. *J. Chem. Phys.* **1993**, *98*, 5648−5652. (b) Lee, C.; Yang, W.; Parr, R. G. Development of the Colle-Salvetti correlation-energy formula into a functional of the electron density. *Phys. Rev. B: Condens. Matter Mater. Phys.* **1988**, *37*, 785−789.

(24) Schäfer, A.; Horn, H.; Ahlrichs, R. Fully optimized contracted Gaussian basis sets for atoms Li to Kr. *J. Chem. Phys.* **1992**, *97*, 2571−2577.

(25) Schäfer, A.; Huber, C.; Ahlrichs, R. Fully optimized contracted Gaussian basis sets of triple zeta valence quality for atoms Li to Kr. *J. Chem. Phys.* **1994**, *100*, 5829−5835.

(26) Neese, F.; Wennmohs, F.; Hansen, A.; Becker, U. Efficient, approximate and parallel Hartree−Fock and hybrid DFT calculations. A 'chain-of-spheres' algorithm for the Hartree−Fock exchange. *Chem. Phys.* **2009**, *356*, 98−109.

(27) Weigend, F.; Ahlrichs, R. Balanced basis sets of split valence, triple zeta valence and quadruple zeta valence quality for H to Rn: design and assessment of accuracy. *Phys. Chem. Chem. Phys.* **2005**, *7*, 3297−3305.

(28) *Manual for ORCA, Version 2.8*; Institut für Physikalische und Theoretische Chemie, Universität Bonn: Bonn, 2010; p 453.

(29) Mungwe, N.; Swarts, A. J.; Mapolie, S. F.; Westman, G. Cationic palladacycles as catalyst precursors for phenyl acetylene polymerization. *J. Organomet. Chem.* **2011**, *696*, 3527−3535.

(30) Shan, W. G.; Bian, G. F.; Su, W. K.; Liang, X. R. A facile one-pot preparation of isothiocyanates from N-formamides and sulfur powder with bis(trichloromethyl) carbonate. *Org. Prep. Proced. Int.* **2004**, *36*, 283−286.